J Mater Sci (2007) 42:298–301
DOI 10.1007/s10853-006-1012-9

Dielectric properties of $Pb(Zn_{1/3}Ta_{2/3})O_3$-introduced $(Ba,Pb)TiO_3$ ceramic system

Kyung-Han Seo · Nam-Kyoung Kim

Received: 16 August 2004 / Accepted: 23 September 2005 / Published online: 30 November 2006

Abstract Ceramic powders of the $Pb(Zn_{1/3}Ta_{2/3})O_3$-introduced $BaTiO_3$–$PbTiO_3$ system were prepared using a B-site precursor method. Perovskite formation tendencies of the system compositions were determined by X-ray diffraction. Weak-field low-frequency dielectric properties of the sintered ceramics were investigated. Dielectric constant spectra were further analyzed in terms of diffuseness. Internal microstructures of the ceramics were also examined.

Introduction

Barium titanate and lead titanate, $BaTiO_3$ and $PbTiO_3$ (BT and PT), are well-investigated perovskites of a tetragonal symmetry (at room temperature). BT and PT can be readily prepared by solid-state reactions between constituent chemicals. Dielectric constant spectra of the two compounds are quite sharp with little frequency-dependent relaxation. Dielectric maximum temperatures of the BT–PT binary system were in the range of 120–490 °C.

Compared with BT and PT, lead zinc tantalate $Pb(Zn_{1/3}Ta_{2/3})O_3$ (PZT) is a much less studied composition. Formation of a perovskite structure in PZT has not been accomplished by any means so far [1–6]. Instead, only a pyrochlore structure resulted. However, preparation of perovskite lead zinc niobate $Pb(Zn_{1/3}Nb_{2/3})O_3$ (PZN) has been successful, when high pressures [7, 8], flux-assisted crystal growth [9–11], or mechanochemical reaction routes [12, 13] were employed. Therefore, the inability to synthesize the perovskite PZT can be attributed, at least in part, to the smaller electronegativity difference [14] of Ta–O (as compared with that of Nb–O in PZN), which would favor the formation of the pyrochlore of higher covalency. The failure can also be attributed to the somewhat larger size [15] of the $Zn_{1/3}Ta_{2/3}$ complex for the sixfold lattice sites formed by oxygen octahedra. It should be noted that PZT in the present paper does not stand for $Pb(Zr,Ti)O_3$, but rather for a Ta-analog of $Pb(Zn_{1/3}Nb_{2/3})O_3$. Nor does the expression of $Pb(Zn_{1/3}Ta_{2/3})O_3$ (or PZT as well) indicate the formability of a perovskite structure.

In the present study, 20 mol% PZT was introduced into the $(Ba,Pb)TiO_3$ perovskite system and the effects of the compositional modification on the perovskite formation and dielectric properties were investigated. In the powder synthesis, B-site precursor compositions were separately prepared, prior to reactions with the remaining components. The two-stage reactions of a B-site precursor method [16, 17] (a more comprehensive term for the so-called columbite process [18]) were employed to suppress the formation of pyrochlore, the presence of which (even in small quantities) has been well documented to be detrimental to dielectric properties [1, 19, 20].

Experimental procedure

The 20 mol% $Pb(Zn_{1/3}Ta_{2/3})O_3$-modified $(Ba,Pb)TiO_3$ system can be formulated as $0.2Pb(Zn_{1/3}Ta_{2/3})O_3$–

K.-H. Seo · N.-K. Kim (✉)
Department of Inorganic Materials Engineering,
Kyungpook National University, Daegu 702-701, Korea
e-mail: nkkim@knu.ac.kr

$(0.8–x)BaTiO_3–xPbTiO_3$, i.e., $(Pb_{0.2+x}Ba_{0.8–x})[(Zn_{1/3}Ta_{2/3})_{0.2}Ti_{0.8}]O_3$ or 0.2PZT–(0.8–*x*)BT–*x*PT in short. Several compositions (ranging from $x = 0.0$ to $x = 0.8$ at regular intervals of 0.2) of the system were selected for investigation. Starting materials were high-purity chemicals of PbO (99.5%), $BaCO_3$ (99.9%), ZnO (99.8%), Ta_2O_5 (99.9%), and TiO_2 (99.9%).

As the B-site compositions of $[(Zn_{1/3}Ta_{2/3})_{0.2}Ti_{0.8}]O_2$ were identical throughout the compositions (regardless of *x*), the precursor powders were prepared as a common batch by wet-milling (ZrO_2 media) under alcohol for 12 h of the required chemicals in stoichiometric proportions, followed by drying and calcination at 1,200 °C for 2 h in a covered alumina crucible. The steps from milling to calcination were repeated one more time under identical conditions to promote phase development. The precursor powders were then mixed with appropriate amounts of PbO and $BaCO_3$, and calcined at 800–850 °C for 2 h. The calcination procedures were again repeated one more time at 800–1,000 °C with intermediate milling and drying stages. Calcined powders were examined by X-ray diffraction (XRD, CuKα, 30 kV, 30 mA, scanning speed = 4°2θ/min) after each heat-treatment stage to identify the phases formed. Thus-prepared 0.2PZT–(0.8–*x*)BT–*x*PT powders (with the addition of 2 wt% polyvinyl alcohol as binder) were pressed into pellet forms (10 mm in diameter and ~2 mm in thickness), followed by further isostatic compaction at ~100 MPa. The samples were embedded in identical composition powders and fired for 1 h at 1,250–1,300 °C in a multiple-enclosure inverted-crucible setup [21]. Major faces of the sintered ceramics were ground/polished to attain parallel sides, onto which Au was sputtered as electrical contacts. Low-frequency (1–1,000 kHz) dielectric constant values of the ceramics were measured under weak-field (1 V_{rms}/mm) conditions, while the temperature was lowered. The samples were fractured, Au-coated, and the internal structures were examined using a scanning electron microscope.

Results and discussion

An X-ray result of the B-site precursor $[(Zn_{1/3}Ta_{2/3})_{0.2}Ti_{0.8}]O_2$ powder is illustrated in Fig. 1, along with the profiles of $[(Zn_{1/3}Ta_{2/3})_{1/2}Ti_{1/2}]O_2$ and TiO_2 rutile (ICDD Nos. 39-292 and 21-1276, respectively) for comparison. Angular positions of the precursor powder were located between respective reflections of $[(Zn_{1/3}Ta_{2/3})_{1/2}Ti_{1/2}]O_2$ and TiO_2, indicating mutual dissolution of the two components into each other. Therefore, it can be concluded that the structure of the synthesized powder is a monophasic solid solution formed between the two rutiles. Theoretical resolution of the precursor composition $[(Zn_{1/3}Ta_{2/3})_{0.2}Ti_{0.8}]O_2$ as $0.4[(Zn_{1/3}Ta_{2/3})_{1/2}Ti_{1/2}]O_2 + 0.6TiO_2$ validates this conclusion. Moreover, positions of the precursor pattern were slightly closer to those of TiO_2, confirming the nominal ratio of $[(Zn_{1/3}Ta_{2/3})_{1/2}Ti_{1/2}]O_2$:$TiO_2$ = 4:6.

X-ray diffractograms of the 0.2PZT–(0.8–*x*)BT–*x*PT system are contrasted in Fig. 2, in which only a perovskite structure was observed throughout the compositions. Hence, the perovskite yields of $I_{perov.}/(I_{perov.} + I_{pyro.})$ were 100% in spite of the incorporation of 20 mol% PZT of pyrochlore-prone nature. The pattern of $x = 0.0$ was (pseudo)cubic, whereas several reflections started to split as the values of *x* increased, leading to a morphotropic phase boundary around $x = 0.2$. Development of the tetragonal symmetry was most pronounced at $x = 0.8$. It is interesting to note that the tetragonal symmetry of BT was completely diluted at $x = 0.0$ (0.2PZT–0.8BT) by the incorporation of 20 mol% PZT, whereas that of PT still survived at the same condition of $x = 0.8$ (0.2PZT–0.8PT). This

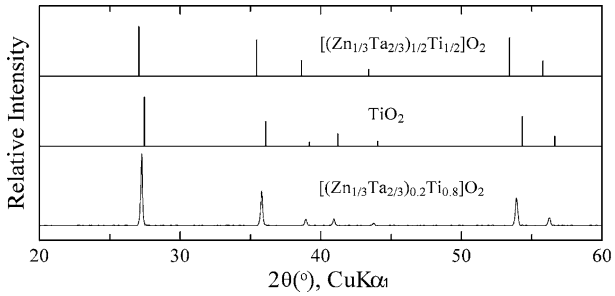

Fig. 1 XRD result of the B-site precursor composition $[(Zn_{1/3}Ta_{2/3})_{0.2}Ti_{0.8}]O_2$, as compared with the profiles of rutile $[(Zn_{1/3}Ta_{2/3})_{1/2}Ti_{1/2}]O_2$ and TiO_2

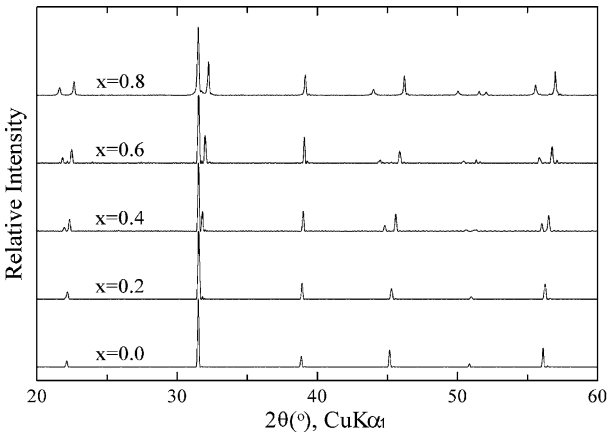

Fig. 2 XRD patterns of the 0.2PZT–(0.8–*x*)BT–*x*PT system

difference can obviously be attributed to the greater tetragonality value of PT (c/a = 1.065, ICDD No. 6-452), as compared with 1.011 of BT (ICDD No. 5-626). Relative densities of the sintered ceramics were 94.0–97.5% of theoretical.

Dielectric constant spectra of the system ceramics are displayed in Fig. 3. Dependence of the dielectric maximum temperature upon composition is also plotted in the inset. At $x = 0.0$, the spectra were rather broad, with the maximum values of 7,150 (–114 °C), 6,550 (–97 °C), 5,520 (–72 °C), and 3,860 (–43 °C) at 1, 10, 100, and 1,000 kHz, respectively. A very strong shift in the peak temperatures (71 °C over the 1–1,000 kHz range) at $x = 0.0$ is noticeable. Moreover, the values at 1 MHz showed a quite broad plateau, which might be quite useful for practical applications. At $0.4 \leq x$, however, the phase transition modes were quite sharp with almost negligible frequency dependence. For instance, the maximum values of $x = 0.6$ were 14,100, 14,000, 13,800, and 13,700 all at 275 °C at the four frequency decades.

The dielectric constant spectra in the paraelectric temperature range were analyzed in terms of diffuseness. Two relative measures of the diffuseness characteristics are the diffuseness exponent (γ) and the degree of diffuseness (C/K_{max}), details of which can be found elsewhere [4, 5, 22–25]. Intermediate results are presented in Fig. 4, where final values of the two parameters are included in the inset. As shown, the two parameters were considerably larger at BT-rich compositions, whereas the values decreased almost continuously with increasing x (PT fraction). The overall decreases in the two parameters are, of course, intimately associated with the dielectric constant spectra (Fig. 3).

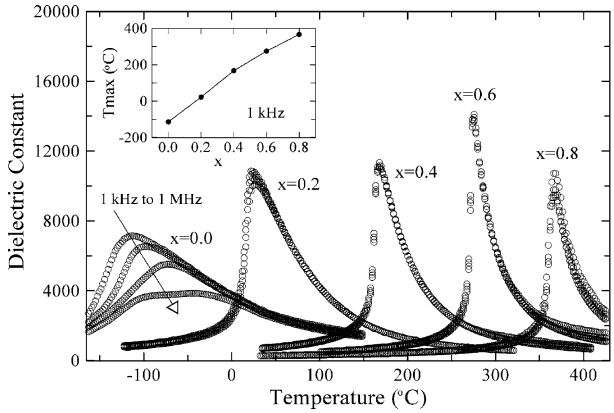

Fig. 3 Dielectric constant spectra of the system ceramics. Variation of the dielectric maximum temperature with compositional change is included in the inset

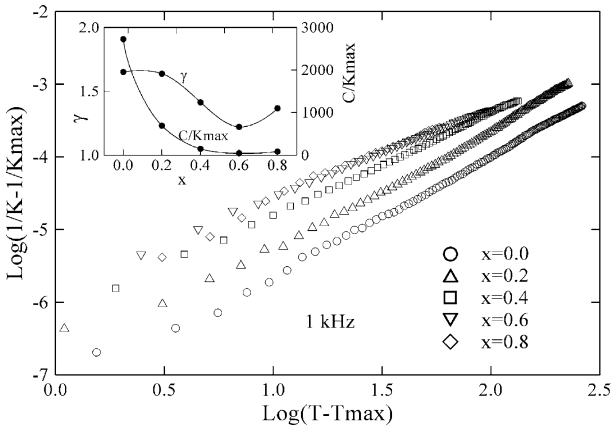

Fig. 4 $\mathrm{Log}(1/K–1/K_{max})$ versus $\log(T–T_{max})$ plots, with determined values of the diffuseness exponent (γ) and degree of diffuseness (C/K_{max}) plotted in the inset

A representative microstructure ($x = 0.4$) of the fractured surface is shown in Fig. 5. Typical morphology of well-developed multifaceted polyhedral perovskite grains with little porosities is observable. Moreover, the fracture modes were preferentially intergranular. Other compositions of the system also showed similar internal structures, with average grain sizes of 2–3 μm.

Summary

A fixed amount of 20 mol% $Pb(Zn_{1/3}Ta_{2/3})O_3$ was substituted into the $(Ba,Pb)TiO_3$ system and subsequent properties were characterized. Only a rutile solid solution was identified in the common B-site precursor composition of $[(Zn_{1/3}Ta_{2/3})_{0.2}Ti_{0.8}]O_2$. After the reactions of the precursor powder with the remaining components, only a perovskite structure was detected throughout the system compositions. (Pseudo)cubic

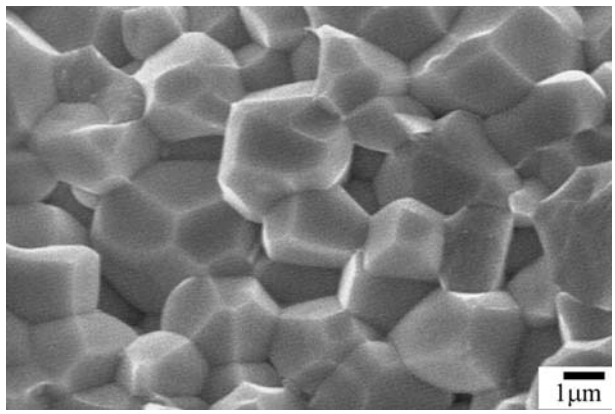

Fig. 5 Fractomicrograph of $x = 0.4$

symmetries developed at low values of x (i.e., BT-rich compositions), whereas tetragonal symmetries became pronounced with increasing x. Dielectric constant spectra of the BT-rich compositions were quite broad and exhibited frequency-dependent dielectric relaxation. In contrast, the spectra became quite sharp with little dispersion at high values of x. The dielectric maximum temperatures of the ceramics increased almost linearly with the compositional change: –114 °C (x = 0.0) to 367 °C (x = 0.8) at 1 kHz. Magnitudes of the two diffuseness parameters decreased continuously with increasing x in general. Microstructures of the sintered ceramics were composed of well-developed perovskite grains of 2–3 μm in size.

Acknowledgement This study was supported by a grant from the Korea Science and Engineering Foundation (KOSEF) through the Basic Research Program (R05-2003-000-10068-0).

References

1. Shrout TR, Halliyal A (1987) Am Ceram Soc Bull 66:704
2. Ling HC, Yan MF, Rhodes WW (1989) Ferroelectrics 89:69
3. Ahn B-Y, Kim N-K (2000) Mater Res Bull 35:1677
4. Lim S-M, Kim N-K (2000) J Mater Sci 35:4373
5. Chae M-C, Lim S-M, Kim N-K (2000) Ferroelectrics 242:25
6. Kim J-S, Kim N-K, Kim H (2003) J Am Ceram Soc 86:929
7. Matsuo Y, Sasaki H, Hayakawa S, Kanamaru F, Koizumi M (1969) J Am Ceram Soc 52:516
8. Ravindranathan P, Srikanth V, Komarneni S, Bhalla AS (1996) Ferroelectrics 188:135
9. Bokov VA, Myl'nikova IE (1961) Sov Phys-Solid State 2:2428
10. Yokomizo Y, Takahashi T, Nomura S (1970) J Phys Soc Jpn 28:1278
11. Park CS, Lim KY, Choi DY, Chung SJ (1998) J Kor Phys Soc 32(Suppl):S974
12. Wang J, Wan D, Xue J, Ng WB (1999) J Am Ceram Soc 82:477
13. Wang J, Xue J, Wan D (2000), Solid State Ionics 127:169
14. Smith WF (1990) In: Principles of materials science and engineering (2nd edn.). McGraw-Hill, Singapore, p 37
15. Shannon RD (1976) Acta Crystallogr A32: 751
16. Lee B-H, Kim N-K, Kim J-J, Cho S-H (1998) Ferroelectrics 211:233
17. Ananta S, Thomas NW (1999) J Eur Ceram Soc 19:155
18. Swartz SL, Shrout TR (1982) Mater Res Bull 17:1245
19. Chen J, Gorton A, Chan HM, Harmer MP (1986) J Am Ceram Soc 69:C303
20. Yan MF, Ling HC, Rhodes WW (1989) J Mater Res 4:930
21. Chae M-C, Kim N-K, Kim J-J, Cho S-H (1998) Ferroelectrics 211:25
22. Uchino K, Nomura S (1982) Ferroelectrics Lett 44:55
23. Butcher SJ, Thomas NW (1991) J Phys Chem Solids 52:595
24. Kuwabara M, Takahashi S, Goda K, Oshima K, Watanabe K (1992) Jpn J Appl Phys 31:3241
25. Ahn B-Y, Kim N-K (2000) J Am Ceram Soc 83:1720